Arch. Mech., 51, 6, pp. 865–884, Warszawa, 1999

Estimation and prediction of local strain-induced martensitic transformation

Y. TOMITA ([1]) and Y. SHIBUTANI ([2])

([1]) *Graduate School of Science and Technology, Kobe University, Kobe, Japan*

([2]) *Graduate School of Engineering, Osaka University, Osaka, Japan*

UNIAXIAL TENSION TESTS were performed under constant strain rate and different environmental temperatures from 77 K to 373 K to identify the concrete form of the constitutive equation for TRIP steels. Subsequently, a new experimental procedure based on microhardness testing which provides local information regarding the transformation has been proposed. To elucidate the dependence of the martensitic transformation on the nonuniform deformation and consequently, to validate the proposed constitutive equation, the volume fraction of the martensite phase is predicted and measured by using computational simulation and experimental procedures, respectively, for the uniaxial tension of the bars with a ringed notch. Good correspondence between the local volume fraction of the martensite phase around the notch obtained by both methods verifies the validity of the proposed constitutive equation for the nonuniform deformation behavior. It has been further clarified that the development of the martensitic phase may relieve the strain localization around the notch tip and subsequently, will increase the energy absorption which is accompanied by an improvement in the toughness.

1. Introduction

MARTENSITIC TRANSFORMATION of transformation-induced plasticity (TRIP) steel is observed during large deformation in the low-temperature range [1]. Owing to the duplex phase of austenite and martensite, the TRIP steel functionally improves the ductility and fracture toughness. However, strain and temperature dependence on the deformation behavior and microscopic transformation mechanism are quite complicated and it may be very difficult to determine a method for the improvement of the mechanical properties merely by experiments. To date, the constitutive equation accounting for the temperature and strain effect on the martensitic transformation [2] and its generalization to account for the stress state [3], strain rate sensitivity [4], and the stress state for stacking fault energy [5] have

been proposed and computational simulations have been conducted to exemplify the transformation behavior and the mechanisms for improving the mechanical properties through the forming processes. For the transformation behavior which is very sensitive to the orientation of the crystalline direction, however, the validity and limitation of the applicability of the constitutive equation should be examined.

With regard to the experimental estimation of the volume fraction of martensitc phase, different methods have been employed so far. Among them are X-ray diffraction [6], magnetic [7], density [8] and electrical resistivity [9] methods which are mainly concerned with the estimation of the average volume fraction of the martensite phase over a relatively large area or volume. As indicated by OLSON and COHEN [2], the strain induced transformation is closely related to the local nonuniform deformation; therefore, development of the experimental procedure for the estimation of the local distribution of the martensite phase is indispensable.

In this study, SUS304 steel which is a typical TRIP steel, is employed as the material for the experiments. Through the precise tension tests conducted under the environmental temperature of 77 K to 373 K, the effect of transformation on macroscopic stress-strain relation is clarified. Then, using the magnetic method, the volume fraction of martensite is measured for the specimens at various strain levels, and the relation between the volume fraction of the martensitic phase and strain is established. With these results and the microhardness test, the master curve for volume fraction of martensite vs. microhardness is established for the measurement of the local distribution of martensitic phase. Subsequently, the master curve is used to estimate the local distribution of the martensite phase over the cross-section of the bar with ringed notch under tension with an environmental temperature of 77 K. The results are compared with those obtained by computational simulation and the validity and limitations of the computational simulation are discussed.

2. Uniaxial tension test

Figure 1 shows the equivalent stress-plastic strain relations of the SUS304 stainless steel specimen shown in the inset with chemical composition indicated in Table 1, deformed under average strain rate of 5×10^{-4}/s and environmental temperatures of 373 K, 303 K, 293 K, 273 K, 253 K, 233 K, 213 K, 193 K, 153 K, 113 K and 77 K. Water, ethanol cooled by liquid nitrogen and liquid nitrogen are respectively used as cooling media for the environmental temperatures of 373 K to 273 K, 253 K to 153 K and 77 K. Whereas, liquid nitrogen vapor was used to realize the environmental temperature of 113 K; therefore, the heat conduc-

tion conditions for the case of 113 K could be different from those of the other cases. The black circles in the figure indicate the load maximum points where the instability, in Considere's sense, takes place. After the load maximum point, the nonuniform deformation, i.e., necking, starts with a substantial decrease of the nominal stress. The stress-strain relation for 373 K which is higher than the Md temperature, indicates the stress-strain relation for austenite since the martensitic transformation may not occur. Due to the strengthening mechanism caused by the martensitic transformation, the onset of maximum load is remarkably delayed and as a result, substantial extendibility is realized. Although the temperature of the Ms point for the material is lower than that of liquid nitrogen, very rapid stiffening at the plastic straining is observed due to plastic strain-induced martensitic transformation.

Table 1. Chemical composition of type 304 austenitic stainless

	Stainless Steel (SUS304)									
Element	C	Si	Mn	P	S	Ni	Cr	Mo	N	Nb
wt %	0.076	0.45	1.18	0.028	0.023	8.19	18.22	0.06	0.0786	> 0.01

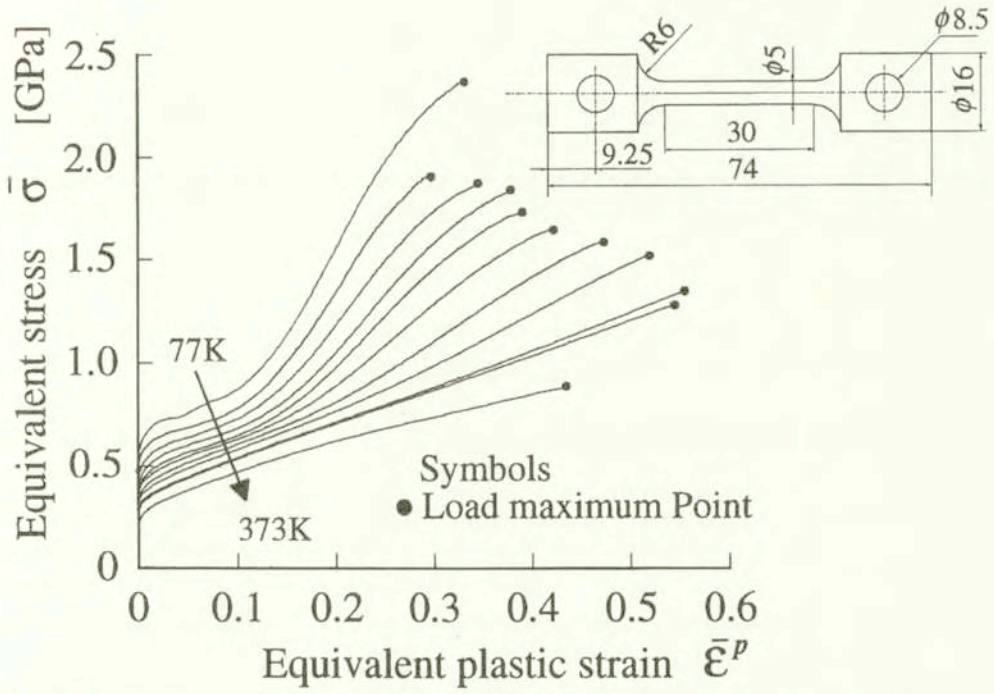

FIG. 1. Equivalent stress $\bar{\sigma}$-plastic strain $\bar{\varepsilon}^p$ relations for SUS304 stainless steel deformed with strain rate 5.0×10^{-4}/s under different environmental temperatures 77–373 K.

The mechanisms for the improvement of ductility can be clarified by investigating Considere's condition for the onset of instability [4]. Due to the strengthening effect of the martensitic transformation, the rate of work-hardening $d\sigma/d\varepsilon$ first increases to a maximum, then decreases due to the saturation of the martensitic transformation, and finally, the front of the curve joins the stress-strain curve. Although, in the low-temperature range, the increase in the work-hardening rate is considerable; the rapid saturation causes a high rate of decrease in work-hardening and a rise in the stress strain curve, which causes the onset of instability in the early stage of deformation. Consequently, to improve the ductility of the material due to martensitic transformation is not simply the increase of the final value of the volume fraction of martensitic phase but the process of martensitic transformation including the effects of strain rate and temperature, which should be accounted for in the design of forming processes. Further discussion on this topic was presented in a separate paper [10]. The slightly different feature observed in the stress-strain relation for 113 K could be attributed to the above mentioned different cooling condition with respect to the other cases.

3. Estimation of volume fraction of martensitic phase by means of microhardness test

The microhardness testing device employed for the present investigation is a dynamic ultramicrohardness testing device (Shimazu DUH-201). A specially designed automatic positioning device and Shimazu DUH-201 consist of an automatic multipoint measuring system which enables the estimation of the hardness distribution over the desired area. The experimental conditions such as holding time, indentation load and surface conditions have been investigated in an earlier work [11].

In order to establish the master curve for the volume fraction of martensitic phase f^m vs. vs microhardness H, circular chips with 0.5 mm thickness made from the uniformly deformed specimen with different plastic strains under liquid nitrogen are prepared. In this investigation, the magnetic permeability method was employed to estimate the magnetization-magnetic field relation [11]. Figure 2 shows the obtained magnetic permeability μ vs. equivalent plastic strain $\bar{\varepsilon}^p$ relation. The volume fraction of the martensite phase should be calculated based on the magnetic permeability for the specimen with 100% volume fraction of martensitic phase. However, since it is very difficult to obtain the specimen with 100% volume fraction of martensitic phase, saturation magnetization method [8] was utilized to estimate the true volume fraction of the martensite phase for the circular chips with 30% plastic strain. The saturation value of magnetization of the martensitic phase can be expressed by $\sigma^m = 214.5 - 3.12(C_r + 0.5N_i)$; C_r, N_i

indicate the weight percentage of individual chemical elements. The corresponding saturation value is $\sigma^m = 144.9$ [emu/g]. Therefore, with estimation value of 30% plastic strain by means of the magnetic permeability method $\sigma^{0.3} = 120$ [emu/g], we can estimate the volume fraction of martensitic phase at 30% plastic strain as $f^m_{0.3} = \sigma^{0.3}/\sigma^m = 0.828$, which will be used to estimate the volume fraction of martensitic phase versus equivalent plastic strain.

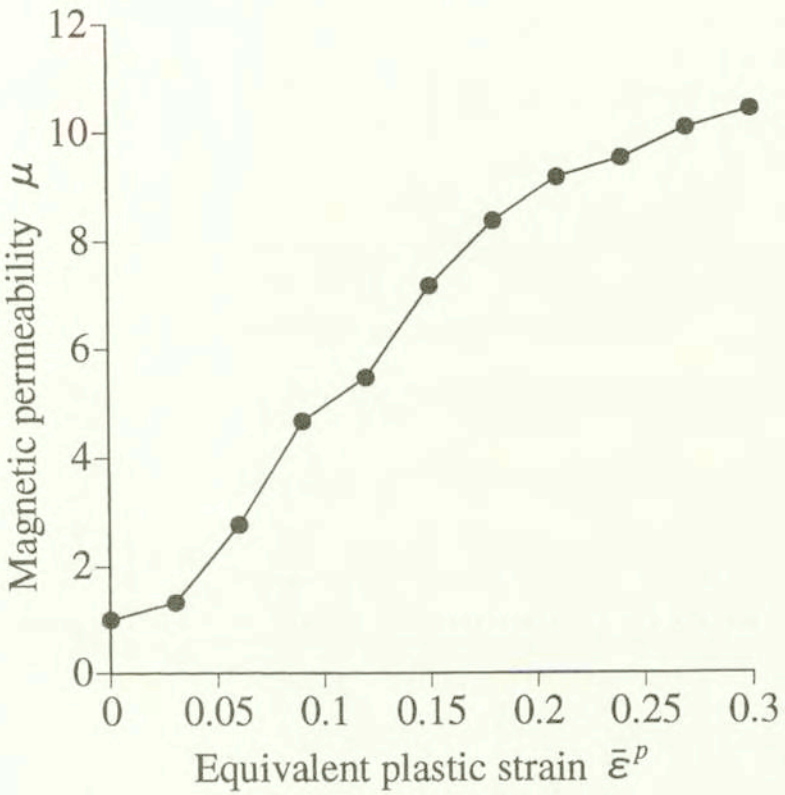

FIG. 2. Magnetic permeability μ vs. equivalent plastic strain $\bar{\varepsilon}^p$.

Thus, the obtained volume fraction of the martensitic phase-equivalent plastic strain is shown in Fig. 3, which exhibits the typical s-shaped curve seen in the volume fraction of martensitic phase vs. plastic strain. The same specimens employed for the above experiment are used to obtain the microhardness vs. equivalent plastic strain relation as shown in Fig. 4. In the figure, microhardness was estimated using three different indentation loads, 196, 490 and 1960 mN. Depending on the relative size of the indent with respect to microstructure of the material, the microhardness changes with the indentation loads. Therefore, in this investigation, depending on the employed indentation load, the corresponding relation will be used for the estimation of the local distribution of the volume

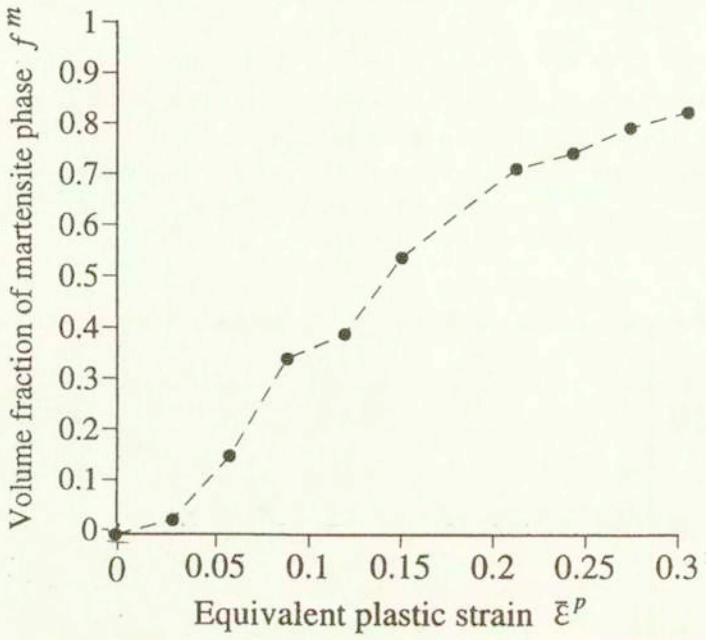

FIG. 3. Volume fraction of martensite phase f^m vs. equivalent plastic strain $\bar{\varepsilon}^p$ relations.

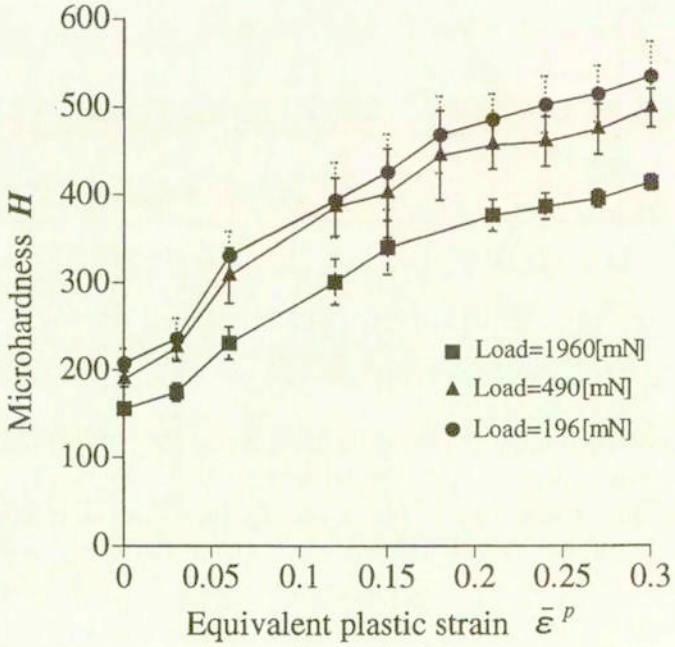

FIG. 4. Microhardness H vs. equivalent plastic strain $\bar{\varepsilon}^p$ relations for three different indentation loads.

fraction of martensitic phase. The master curves for volume fraction of martensitic phase vs. microhardness shown in Fig. 5 can be established by using the relations in Figs. 3 and 4. The corresponding master curve is finally expressed as

$$
\begin{aligned}
(3.1) \qquad f^m &= C_1 H^2 + C_2 H + C_3, \\
P &= \ 196 \text{ mN} : C_1 = 4.25 \times 10^{-6}, C_2 = 3.82 \times 10^{-4}, \ C_3 = 1.20 \times 10^{-1}, \\
P &= \ 490 \text{ mN} : C_1 = 5.83 \times 10^{-6}, C_2 = 1.09 \times 10^{-3}, \ C_3 = 1.90 \times 10^{-2}, \\
P &= 1960 \text{ mN} : C_1 = 5.62 \times 10^{-6}, C_2 = 1.47 \times 10^{-4}, \ C_3 = 1.59 \times 10^{-1}.
\end{aligned}
$$

Equation (3.1) will be fully employed for the estimation of local distribution of volume fraction of the martensitic phase.

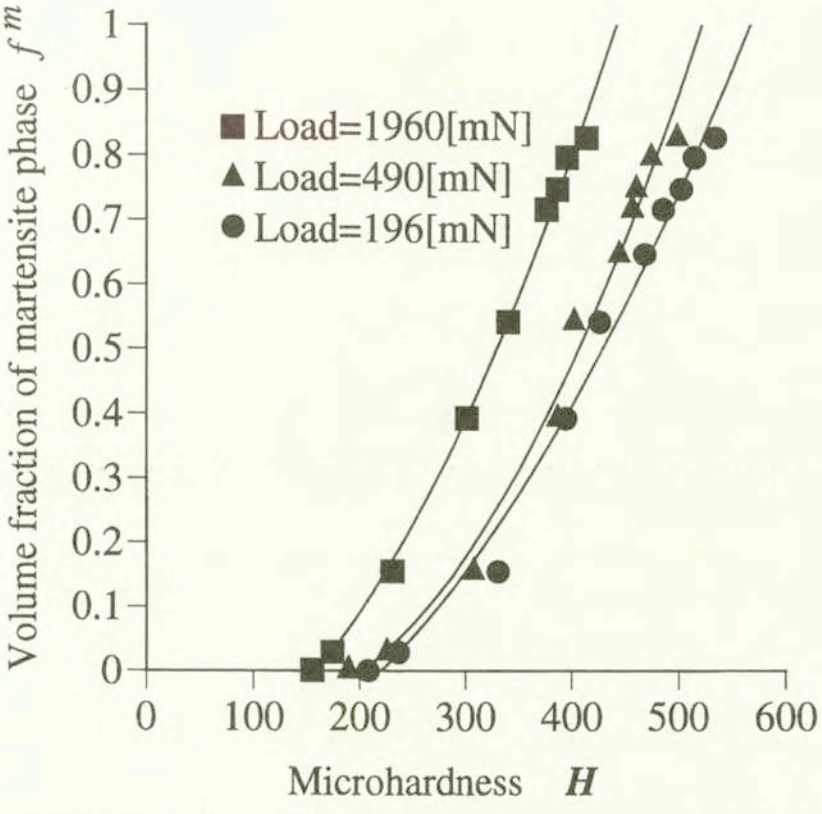

FIG. 5. Volume fraction of martensite phase f^m vs. microhardness H relation for three different indentation loads.

4. Constitutive equation of TRIP steels

For the self-completeness of the paper, a brief explanation of the constitutive equation utilized in this investigation is given. OLSON and COHEN [2] established

a fundamental model for strain-induced martensitic transformation kinetics which can express the temperature dependence of the transformation phenomena. This phenomenological model was constructed under the assumption that the transformation occurred at the intersection of the shear band in the austenite mother phase with a prescribed possibility. STRINGFELLOW *et al.* [3] generalized the Olson and Cohen model so as to include the stress state and the contribution of the martensite phase to the strength. TOMITA and IWAMOTO [4] modified the two models to include the experimental finding that the mode of the deformation behavior is controlled by the shear band mode as the strain rate increases [12]. The rate of increase of the volume fraction of the martensitic phase, $\dot{f}^m$, is given by

$$
\begin{aligned}
\dot{f}^m &= A(1-f^m)\dot{\bar{\varepsilon}}_a^{\text{pslip}}, \\
A &= \alpha\beta n(f^{sb})^{n-1}(1-f^{sb}), \\
\dot{f}^{sb} &= \alpha(1-f^{sb})\dot{\bar{\varepsilon}}_a^{\text{pslip}}, \\
\beta &= \frac{\eta}{\sqrt{2\pi}\sigma_g}\int_{-\infty}^{g}\exp\left\{-\frac{(g'-g_0)^2}{2\sigma_g^2}\right\}dg', \\
g &= -T+g_1\Sigma,
\end{aligned}
\tag{4.1}
$$

where $\dot{\bar{\varepsilon}}_a^{\text{pslip}}$ is the equivalent strain rate of slip deformation in austenite, f^{sb} is the volume fraction of the shear band, β is the probability that an intersection forms a martensitic embryo [3, 4] and n and η are geometric constants. g is the driving force of transformation, g_0 is the mean value of g, g_1 is a constant and σ_g is the standard deviation. α is a parameter related to the stacking fault energy and is a function of temperature T [3], strain rate $\dot{\bar{\varepsilon}}_a^{\text{pslip}}$ [4] and the stress triaxiality parameter $\Sigma = \sigma_{ii}/(3\bar{\sigma})$ [5] as

$$
\alpha = \left(\alpha_1 T^2 + \alpha_2 T + \alpha_3 - \alpha_4\Sigma\right)\left(\frac{\dot{\bar{\varepsilon}}_a^{\text{pslip}}}{\dot{\varepsilon}_r}\right)^M, \tag{4.2}
$$

where M is the strain rate sensitivity exponent, $\alpha_1 - \alpha_4$ are material parameters and $\dot{\varepsilon}_r$ is the reference strain rate. Next, the plastic strain rate $\dot{\varepsilon}_{ij}^p$ is assumed to be the sum of the plastic strain rate $\dot{\varepsilon}_{ij}^{\text{pslip}}$ induced by the slip deformation in austenite and martensite, and $\dot{\varepsilon}_{ij}^{\text{ptrans}}$ induced by the transformation. Furthermore, the transformation plastic strain rate is split into a deviatoric part, $\dot{\varepsilon}_{ij}^{\text{pshape}}$, related to the shape change, and a dilatational part, $\dot{\varepsilon}_{ij}^{\text{pdilat}}$, expressing the volume change. Under the assumptions that the strain rate $\dot{\varepsilon}_{ij}^{\text{pshape}}$ is considered to

be coaxial with deviatoric stress [4] and that $\dot{\varepsilon}_{ij}^{p\text{dilat}}$ can be expressed in terms of the volume change $\Delta\nu$, which has the value of $0.02 - 0.05$ for austenite steel, the plastic strain rate $\dot{\varepsilon}_{ij}^{p}$ can be expressed as

$$
\begin{aligned}
\dot{\varepsilon}_{ij}^{p} &= p_{ij}\dot{\bar{\varepsilon}}^{p} + s_{ij}\Delta\nu\dot{f}^{m}, \\
p_{ij} &= \frac{3\sigma'_{ij}}{2\overline{\sigma}}, \\
s_{ij} &= -p_{ij}\Sigma + \frac{\delta_{ij}}{3}, \\
\dot{\bar{\varepsilon}}^{p} &= \dot{\bar{\varepsilon}}^{p\text{slip}} + R\dot{f}^{m} + \Sigma\Delta\dot{f}^{m}, \\
R &= R_0 + R_1\left(\frac{\overline{\sigma}}{\sigma_a}\right),
\end{aligned}
\tag{4.3}
$$

where $\dot{\bar{\varepsilon}}^{p}$ is the work equivalent measure of the equivalent plastic strain-rate with respect to Mises-type equivalent stress $\overline{\sigma}$, and R is the parameter accounting for the magnitude of shape changes and depends on the stress. σ_a is the initial yield stress of austenite and R_0 and R_1 are constants. The constitutive equation for the stress rate can be established by introducing the plastic strain rate in Eq. (4.3) into the thermoelastic constitutive equation, as discussed by TOMITA and IWAMOTO [4].

Since strain-induced transformation is quite sensitive to temperature, the mechanical characteristics of the material induced by transformation are strongly affected by the temperature change caused by the irreversible work. Consequently, thermocoupled analysis [13] is unavoidable for the prediction of the deformation behavior of TRIP steel. The constitutive equation of a two-phase composite material of austenite including the volume fraction of martensitic phase f^m is established in a manner similar to that described by STRINGFELLOW *et al.* [3], applying Eshelby's theory [14]. The forward gradient method is introduced to improve the computational efficiency. The identification of the material parameters has been done based on the procedure described by STRINGFELLOW *et al.* [3], SHIMIZU [15] and IWAMOTO *et al.* [5]. The material and computational parameters employed in this investigation are shown in Appendix.

5. Estimation of distribution of volume fraction of martensitic phase

The proposed method is applied for the estimation of the distribution of the volume fraction of the martensite phase over the cross-section of the ringed-notched specimen subjected to uniaxial tension under an environmental tempe-

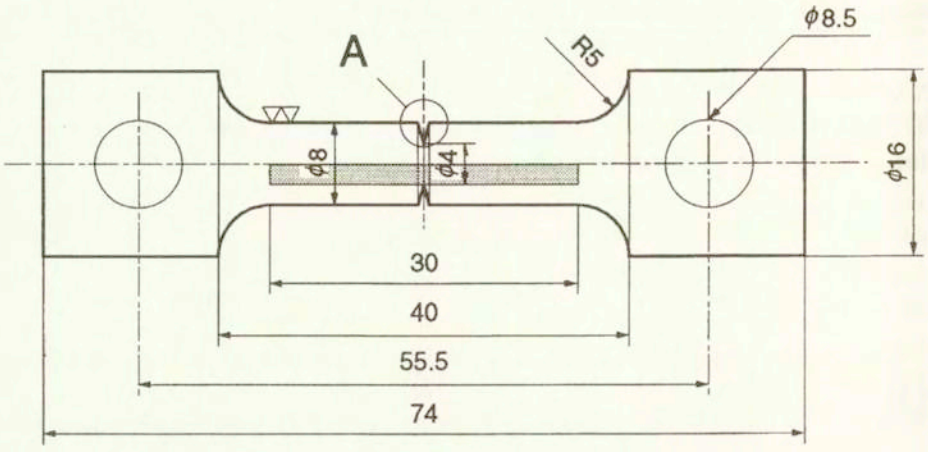

Specimen

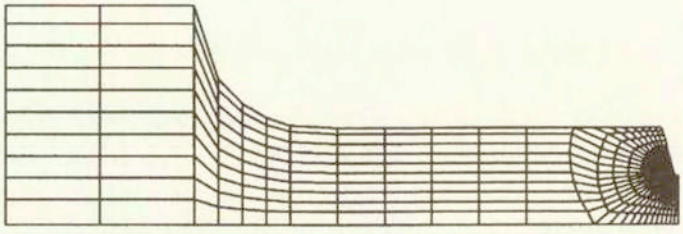

Computational Model

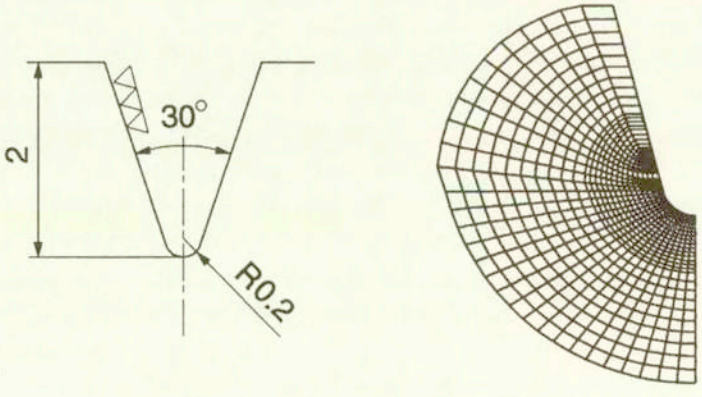

Magnification of A

FIG. 6. Specimen profile and computational model for finite element simulation.

rature of 77 K. The specimen profile and the dimensions are shown in Fig. 6. The average strain rate was set to be 5×10^{-5}/s and the loading was stopped when the end displacement reached 0.32 mm and 0.5 mm. After unloading, the specimens for the measurement of microhardness were prepared by wire cutting and electropolishing with sufficient care to avoid the formation of the surface layer. The automatic estimation of martensitic distribution over the cross-section near the notch tip has been done with three different indentation loads of 1960 mN, 490 mN and 196 mN. Figure 7 indicates the distribution of the volume fraction of the martensitic phase f^m along the radial direction x. The fluctuation of the volume fraction of the martensitic phase due to the nonuniform distribution of the martensite phase is observed. Its amplitude increases as the indentation load decreases which can be attributed to the averaging effect of the martensitic phase. Decrease of the indentation load which causes the decrease of the size of the indent may pick up the more localized distribution of the martensite phase.

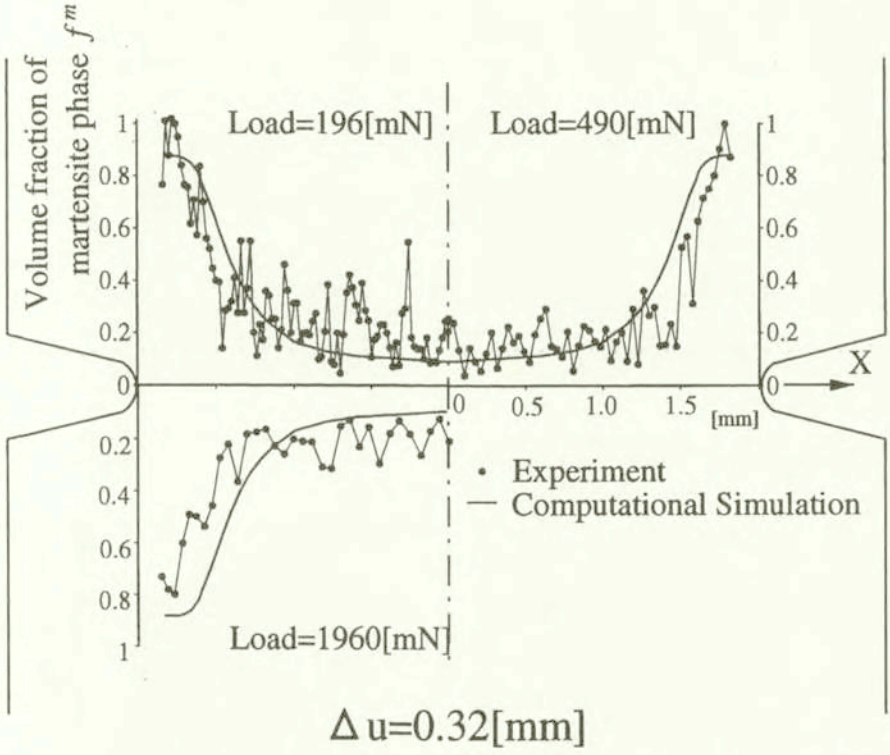

FIG. 7. Distribution of volume fraction of martensitic phase f^m along radial direction estimated using three different indentation loads and that estimated by computational simulation.

Figure 8 indicates the distribution of the volume fraction of the martensite phase f^m over the cross-section near the notch tip. Approximately 2000, 4000 and

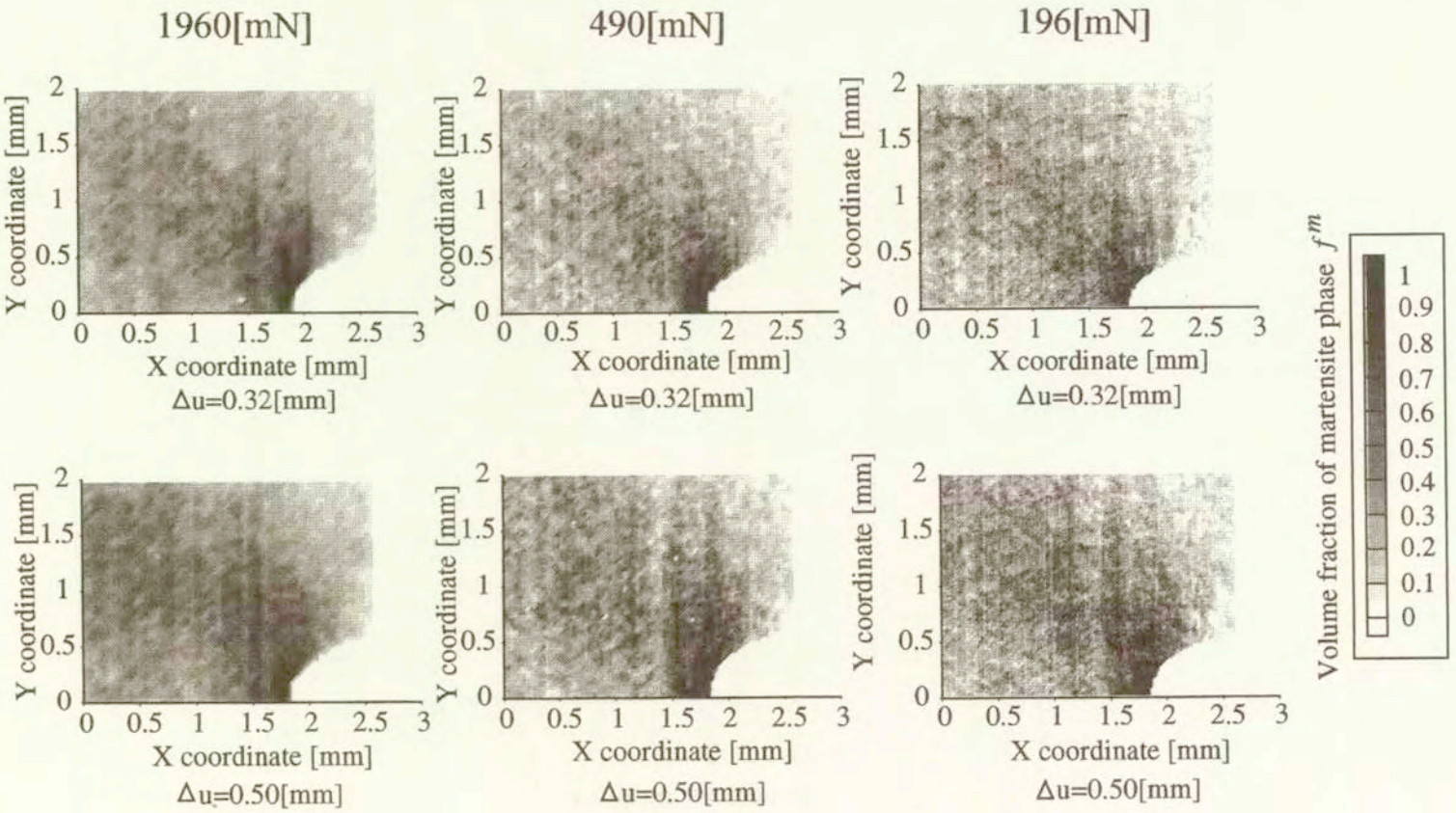

FIG. 8. Distribution of volume fraction of martensitic phase f^m near the notch tip estimated using three different indentation loads.

12000 points have been measured for 1960 mN, 490 mN and 196 mN indentation loads, respectively. In accordance with the local deformation of the notch, the region with high volume fraction of the martensitic phase emanating from the notch tip, spread in approximately 45° direction to the tension axes, which indicates that the martensitic transformation substantially depends on the slip deformation of the crystals [16]. By increasing the number of indentation points and decreasing the indentation load, the clearer distribution of the martensitic phase can be revealed. Due to the strain localization around the notch tip, the region with low martensitic transformation can be observed along the ligament direction of the notch root. Furthermore, the results extract the nonuniform transformation behavior depending on the crystalline direction in the multicrystal with average grain size, 100 μm. Thus, by increasing the number of indentation points, the clearer local information on the transformation can be obtained.

To examine the applicability of the constitutive equation for the prediction of the transformation behavior of TRIP steels, computational simulation has been performed for the specimen modeled by the finite element discretization shown in Fig. 6. Figures 7 and 9 indicate the distribution of volume fraction of martensitic phase f^m predicted by computational simulation and estimated by an experimental method. Apart from the fluctuation of the distribution of the volume fraction of the martensitic phase, a very clear correspondence is seen for both results, which implies the applicability of the constitutive equation for the estimation of the volume fraction of the martensite phase created by the highly nonuniform deformation. However, the results also indicate the limitation of the computational simulation with the constitutive equation developed, based on the volume fraction of the martensitic phase for problems with highly-localized deformation behavior. Therefore, a different type of transformation model which enables the estimation of the local martensite phase should be incorporated; this will be our future work.

Thus, the proposed method of estimation of local distribution of the volume fraction of the martensitic phase clarifies the validity of the prediction of the average martensitic phase distribution based on the phenomenologically developed constitutive equation to some extent, so that we will further discuss the deformation behavior of ringed notched bars. Figure 10 shows the evolution of the volume fraction of martensitic phase with the deformation under the environmental temperatures of 77 K and 293 K. A high volume fraction of the martensite phase is observed during the earlier stage of deformation at 77 K as compared with the case at 293 K, which can be explained by the following distribution of equivalent plastic strain $\bar{\varepsilon}^p$ and triaxiality factor Σ for the respective temperatures, which are shown in Fig. 11. In both cases, the magnitude of plastic equivalent strain is insensitive to the environmental temperature, so that it is recognized that the strong dependence of the probability that an intersection forms a martensitic

FIG. 9. Comparison between distribution of volume fraction of martensite phase estimated experimentally (upper) and by computational simulation (lower).

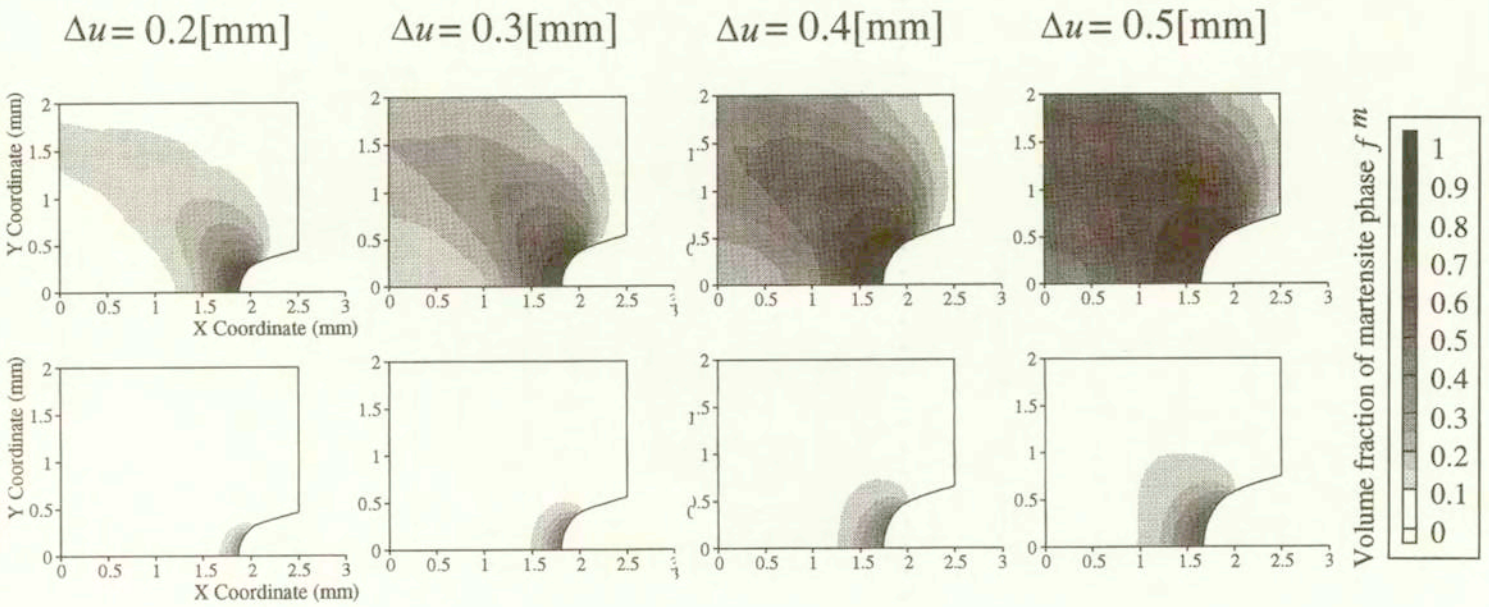

FIG. 10. Distribution of volume fraction of martensite phase f^m for environmental temperatures of 77 K and 293 K estimated by computational simulation.

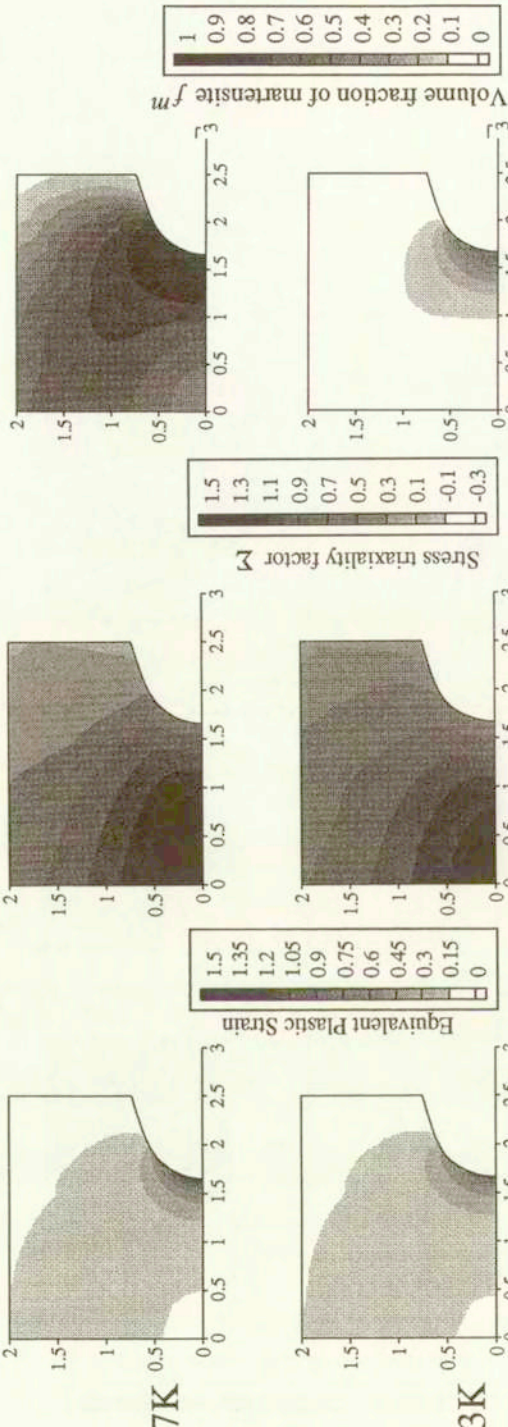

FIG. 11. Distribution of equivalent strain $\bar{\varepsilon}^p$, triaxiality parameter Σ and volume fraction of martensite phase f^m.

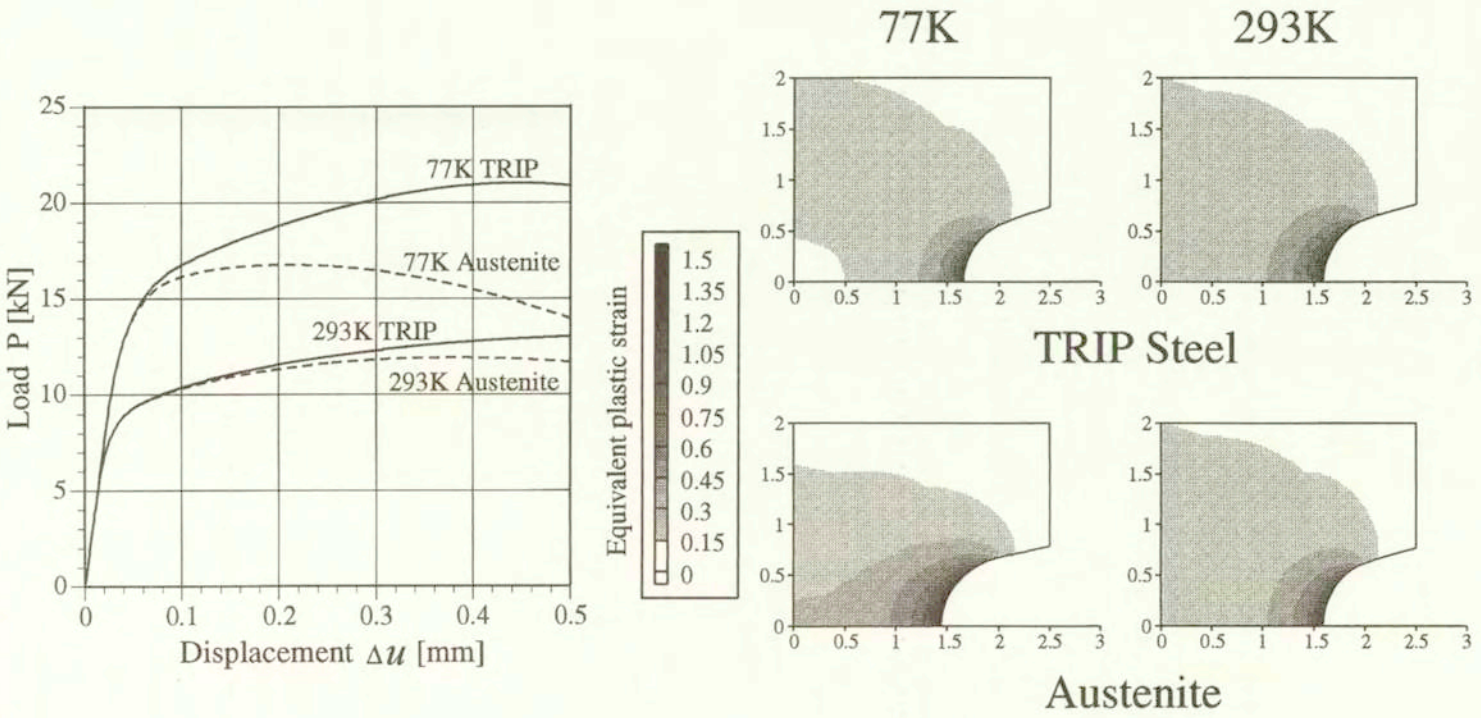

FIG. 12. (a) Load vs. displacement Δu relation and (b) equivalent plastic strain $\bar{\varepsilon}^p$ distribution for environmental temperatures of 77 K and 293 K. For the sake of comparison, the results for the nontransforming case, austenite, are also indicated.

embryo, in other words, the driving force to transformation, on the temperature, substantially affects the transformation.

Figure 12 indicates the load P and displacement Δu relations for the uniaxial tension of the notched specimens deformed under different environmental temperatures. For the purpose of comparison, the nontransforming case, austenite, is also shown. For the low- temperature case, there is a remarkable increase of force due to transformation so that the work required for the deformation increases, which is attributable to the distributing effect by the strengthening caused by martensitic transformation near the notch tip, which is indicated in the plastic equivalent strain distribution. Thus, martensitic transformation may contribute toward the increase in energy absorption from the outside, which yields the improvement of toughness.

6. Conclusion

In this study, through the precise tension tests conducted under the environmental temperatures of 77 K to 373 K, the effect of transformation on the macroscopic stress-strain relation and the improvement mechanism of ductility have been clarified. Then, with the volume fraction of martensite phase estimated using the magnetic method and microhardness measured by employing ultramicrohardness tester, the master curves for volume fraction of martensite phase vs. microhardness for various indentation loads have been established for the measurement of local distribution of volume fraction of the martensitic phase. Subsequently, the established master curves were employed for the estimation of the local distribution of the martensite phase over the cross-section of a ring-notched bar under tension. The results were compared with those obtained by computational simulation with a phenomenologically developed constitutive equation, and the validity and the limitation of the computational simulation have been clarified. By the computational simulation of different environmental temperatures, it has been clarified that the improvement of energy absorption due to the distributing effect of a highly deformed region by the martensitic transformation contributes toward the improvement of ductility. Furthermore, it is expected that the experimental method with low indentation load will enable the estimation of the highly localized distribution of the volume fraction of the martensitic phase.

Acknowledgments

Financial support from the Ministry of Education of Japan is gratefully acknowledged. I wish to thank Mr. T. IWAMOTO, Research Associate of Hiroshima University, for valuable discussions and graduate students Messrs. T. OGAWA,

A. TANIYAMA, M. SHIMIZU and H. SAKAUE, Kobe University, for assistance with the calculations and experiments.

Appendix

Material parameters at temperature employed in the present investigation are summarized. The discussion concerning the identification of material parameters can be found in [3 – 5] and [15].

Stress-strain relation for austenite and martensite phases are

$$\overline{\sigma} = \sigma_y + c_1 \{1.0 - \exp(-c_2\overline{\varepsilon})\}^{c_3}, \qquad \sigma_y = c_4 \exp(-c_5 T),$$

where $c_1 = 1861.0$, $c_2 = 0.628$, $c_3 = 0.748$, $c_4 = 660.0$, $c_5 = 0.0027$ with elastic modulus $E_a = 215.7 - 0.0692T$ (GPa) and Poisson's ratio $\nu = 0.3$ for austenite phase and $c_1 = 1191.0$, $c_2 = 1.33$, $c_3 = 0.540$, $c_4 = 1056.0$, $c_5 = 0.0013$ with elastic modulus $E_m = 237.3 - 0.0692T$ (GPa) and Poisson's ratio for martensite phase.

Evolution of volume fraction of martensitic phase is indicated as Eqs. (4.1) and (4.2) with material parameters $\eta = 4.5$, $M = 0.013$, $\dot{\varepsilon}_r = 5.0 \times 10^{-4}$/s, $\alpha_1 = 0.0$, $\alpha_2 = -7.92 \times 10^{-2}$, $\alpha_3 = 27.1$, $\alpha_4 = 10.23$ for $T \geq 273$ K. The standard deviation σ_g, mean value g_0 and constant g_1 are 17.0, -276.0 and 28.7, respectively [3 –5].

Constitutive equation for plastic strain rate is expressed as in Eq. (4.3) with $R_0 = 0.02$, $R_1 = 0.02$ and $\Delta\nu = 0.02$.

Additional parameters are density $\rho = 0.78 \times 10^4$ (Kg/m^3), specific heat $c = 0.46 \times 10^3$ (J/kg· K), thermal conductivity $\kappa = 16.3$ (W/m· K), heat transfer coefficient with air $h = 25.0$ (W/m^2· K), thermal expansion $\alpha = 17.3 \times 10^{-6}$/K and latent heat $l_r = -1.50 \times 10^4$ (J/kg).

References

1. Y. TAMURA, *TRIP Steels* (in Japanese), Steel and Iron, 56–3, 429–445, 1979.
2. G.B. OLSON and M. COHEN, *Kinematics of strain-induced martensitic nucleation*, Metall Trans. **A**, 6, 791–795, 1975.
3. R.G. STRINGFELLOW, D.M. PARKS and G.B. OLSON, *A constitutive model for transformation plasticity accompanying strain-induced martensitic transformation in metastable austenitic steels*, Acta Metall, **40**, 1703–1716, 1992.
4. Y. TOMITA and T. IWAMOTO, *Constitutive modeling of TRIP steel and its application to the improvement of mechanical properties*, Int. J. Mech. Sci., **37**, 1295–1305, 1995.
5. T. IWAMOTO, T. TSUTA and Y. TOMITA, *Investigation on deformation mode dependence of strain-induced martensitic transformation in TRIP steels and modeling of transformation kinetics*, Int. J. Mech. Sci., **40**, 173–182, 1998.

6. J. DURNIN and K.A. RIDAL, *Determination of retained austenite in steel by X-ray diffraction*, J. Iron & Steel Institute, **206**, 60–67, 1968.

7. G.C. CURTIS and J. SHERWIN, *Magnetic method for the estimation of ferrite in stainless steel welds*, British J. Applied Physics, **12**, 344–345, 1961.

8. T TANAKA and K. HOSHINO, *Measurement of strain-induced martensitic phase* (in Japanese), Nisshin Seiko Technical Report **52**, 36–47, 1985.

9. A. TAKIMOTO, T. INOUE and S. SHOUDA, *Relationship between the electrical resisitivity and the volume fraction of martensite induced by quenching and deformation* (in Japanese), J. Japan Inst. Metals. **49**, 5, 313–319, 1985.

10. Y. TOMITA and T. IWAMOTO, *Computational simulation of enhancement of ductility in TRIP steels due to environmental temperature control during deformation processes*, Proc. Plasticity'95, 331–334, 1995, Gordon and Breach.

11. Y. SHIBUTANI, A. TANIYAMA, Y. TOMITA and T. ADACHI, *Measurement of local strain-induced martensitic phase transformation by microhardness*, JSMS Japan, **46**, 893–899, 1997.

12. S.S. HECKER, M.G. STOUT, K.P. STAUDHAMMER and J.L. SMITH, *Effect of strain state and strain rate on deformation induced transformation in 304 stainless steel: Part I. Magnetic measurements and mechanical behavior*, Metall Trans **A**, 13, 619–626, 1982.

13. Y. TOMITA, A. SHINDO and S. SASAYAMA, *Plane strain tension of thermo-elasto-viscoplastic blocks*, Int. J. Mech. Sci. **32**, 613–622, 1990.

14. J.D. ESHELBY, *The determination of the elastic field of an ellipsoidal inclusion, and related problems*, Proc. Roy. Soc. Lond., **A241**, 376–396, 1957.

15. M. SHIMIZU, *Evaluation of strain-induced martensitic phase transformation behavior by microhardness and its application to constitutive modeling of TRIP steel* (in Japanese), Solid Mechanics Research Laboratory Report, No. 9802, 1–63, 1998.

16. J.A. VENABLES, *The martensitic transformation in stainless steel*, Phil. Mag., **7**, 35–43, 1964.

Received January 13, 1999.